EUSIPCO 2013 1569742487

INSTANTANEOUS COUNTING OF COMPONENTS IN NONSTATIONARY SIGNALS

N. Saulig[1], *N. Pustelnik*[2], *P. Borgnat*[2], *P. Flandrin*[2], *and V. Sucic*[1]

[1]Faculty of Engineering, University of Rijeka, Croatia
[2] Laboratoire de Physique de l'ENS de Lyon, CNRS (UMR 5672) and Université de Lyon, France

ABSTRACT

In the case of multicomponent AM-FM signals, one bottleneck of mode extraction methods such as synchrosqueezing, is that the reconstruction of the individual components assumes some prior knowledge about their number. In order to reduce supervision, an entropy-based time-frequency method had been previously proposed for automatically estimating the instantaneous number of such components. An analytic treatment of this approach is first given, assessing its performance and limitations, in particular with respect to the Rényi entropy order and the amplitude ratio. Based on this analysis, an iterative strategy is then proposed, that is shown to be effective in the case of unequal amplitudes and applicable to real data signals with a moderate level of noise.

Index Terms— Multicomponent Signal, Time-Frequency Analysis, Rényi Entropy

1. INTRODUCTION

In the case of multicomponent AM-FM signals, estimating the number of components is relevant in several respects. It is known that such a number gives a measure of complexity that can be used for further tasks of detection or classification. Knowing the number of components is also a prerequisite (and, currently, a bottleneck) for powerful methods such as synchrosqueezing [1, 2] in order to achieve unsupervised mode synthesis.

As proposed in [3, 4], the complexity of a signal (i.e., the number of components) can be measured with Rényi entropy. In the case of nonstationary signals, the number of components can vary over time, calling for an instantaneous counting. It has been shown in [5] that this information can be obtained by a short-term version of the Rényi entropy applied to a time-frequency distribution. This appealing new approach offers the user many possibilities of variations, with performance which might depend on factors such as the specific choice of a distribution, the order of the entropy, or the signal structure itself.

The aim of this paper is to further investigate the behavior of the method with respect to the Rényi entropy order and to the ratio of the components amplitudes, in an idealized context of a positive time-frequency energy distribution (e.g., a spectrogram). Based on a simplified, theoretical analysis, we design an algorithm allowing us to obtain an accurate component counting.

More precisely, we recall in Section 2 the relation between the spectrogram, the Rényi entropy, and the number of estimated components. We also propose a simplified model of spectrogram in order to deduce a closed form approximation of this number involving the amplitude values and the entropy order. Based on those results which evidence some limitations of the direct approach when amplitude are unequal, we propose in Section 3 an iterative algorithm to estimate accurately the number of components in such a situation. Section 4 is dedicated to numerical experiments, whereas conclusions and perspectives are given in Section 5.

2. A SIMPLIFIED MODEL

2.1. Rényi entropy and number of components

We consider a multicomponent nonstationary signal which has locally $K(t)$ components at a given time instant t. A simplified model for a slice of width Δt of the spectrogram (or "any" other positive time-frequency energy distribution) of such a signal reads:

$$S(\theta, f) = \mathbf{1}_{\Delta t}(\theta - t) \sum_{k=1}^{K(t)} A_k(t)\, \mathbf{1}_{\Delta f}(f - f_k(t)) \quad (1)$$

for $t - \Delta t/2 \leq \theta \leq t + \Delta t/2$, with Δf the equivalent frequency resolution of the analysis. Each component is supposed to be located at a frequency $f_k(t)$ with an amplitude $A_k(t) > 0$. In order to ensure that the different components do not overlap in the time-frequency plane, we assume further that $\min_{k,k'}\{|f_k(t) - f_{k'}(t)|\} > \Delta f$.

It follows from the above model (1) that

$$E(t) := \int_{t-\frac{\Delta t}{2}}^{t+\frac{\Delta t}{2}} \int_{-\infty}^{+\infty} S(\theta, f)\, d\theta\, df = \Delta t \Delta f \sum_{k=1}^{K(t)} A_k(t) \quad (2)$$

and, if we introduce the normalized quantity $\tilde{S}(\theta, f) :=$

$S(\theta, f)/E(t)$, we have

$$\int_{t-\frac{\Delta t}{2}}^{t+\frac{\Delta t}{2}} \int_{-\infty}^{+\infty} \tilde{S}^{\alpha}(\theta, f)\, d\theta\, df = \frac{(\Delta t \Delta f)^{1-\alpha} \sum_{k=1}^{K(t)} A_k^{\alpha}(t)}{\left(\sum_{k=1}^{K(t)} A_k(t)\right)^{\alpha}}. \tag{3}$$

Therefore, the instantaneous Rényi entropy, which is defined in [5] as a short-term version of the global entropy discussed in [4], can be expressed as:

$$H_{\alpha}(t) := \frac{1}{1-\alpha} \log_2 \int_{t-\frac{\Delta t}{2}}^{t+\frac{\Delta t}{2}} \int_{-\infty}^{+\infty} \tilde{S}^{\alpha}(\theta, f)\, d\theta\, df, \tag{4}$$

with $\alpha \in \mathbb{R}_+^* \backslash \{1\}$. According to (3), this yields to

$$H_{\alpha}(t) = \log_2(\Delta t \Delta f) + \frac{1}{1-\alpha} \log_2 \frac{\sum_{k=1}^{K(t)} A_k^{\alpha}(t)}{\left(\sum_{k=1}^{K(t)} A_k(t)\right)^{\alpha}}. \tag{5}$$

The first term in the r.h.s. of (5) can be seen as the reference entropy of a single component. The number of components estimated with the Rényi entropy follows as [4, 5]

$$N_{\alpha}(t) = 2^{H_{\alpha}(t) - \log_2(\Delta t \Delta f)}, \tag{6}$$

i.e.,

$$N_{\alpha}(t) = \left(\frac{\sum_{k=1}^{K(t)} A_k^{\alpha}(t)}{\left(\sum_{k=1}^{K(t)} A_k(t)\right)^{\alpha}} \right)^{\frac{1}{1-\alpha}} \tag{7}$$

or, equivalently,

$$N_{\alpha}(t) = K(t) \left(\frac{M_{\alpha}(\mathbf{A}(t))}{M_1(\mathbf{A}(t))} \right)^{\frac{\alpha}{1-\alpha}} \tag{8}$$

where, according to [6], $M_{\alpha}(\mathbf{A}(t)) = \left(\frac{1}{K(t)} \sum_{k=1}^{K(t)} A_k(t)^{\alpha} \right)^{\frac{1}{\alpha}}$ denotes the power means of order α, for a given family $\mathbf{A}(t) = (A_1(t), \ldots, A_{K(t)}(t))$ of $K(t)$ non-zero values.

2.2. Interpretation and examples

In order to evaluate the performance of this estimator, we analyse the values taken by $N_{\alpha}(t)$ according to $K(t)$, $A_k(t)$, and α.

2.2.1. When do we have $N_{\alpha}(t) = K(t)$?

It is known [6] that, for any pair of orders r and s such that $r > s > 0$, one has $M_r(\mathbf{A}(t)) \geq M_s(\mathbf{A}(t))$, with equality if and only if $A_1(t) = \ldots = A_{K(t)}(t)$. As a consequence, if $\alpha > 1$, it follows that $M_{\alpha}/M_1 \geq 1$ and, since $\alpha/(1-\alpha) < 0$, that $N_{\alpha}(t) \leq K(t)$. If we rather assume that $\alpha < 1$, one has $M_{\alpha}/M_1 \leq 1$ but, since $\alpha/(1-\alpha) > 0$, one ends up as previously with $N_{\alpha} \leq K(t)$. In summary, assuming continuity for $\alpha = 1$ (value for which the Rényi entropy reduces to the classical Shannon form [4]), one has uniformly for any $\alpha > 0$,

$$N_{\alpha}(t) \leq K(t), \tag{9}$$

with equality if and only if $A_1(t) = A_2(t) = \ldots = A_{K(t)}(t)$, i.e., if all components are of equal spectral amplitude.

On the other hand, depending on the value of α, we have the following relations

$$\begin{cases} \sum_{k=1}^{K(t)} A_k^{\alpha}(t) < \left(\sum_{k=1}^{K(t)} A_k(t)\right)^{\alpha} & \text{if} \quad \alpha > 1, \\ \sum_{k=1}^{K(t)} A_k^{\alpha}(t) > \left(\sum_{k=1}^{K(t)} A_k(t)\right)^{\alpha} & \text{if} \quad \alpha < 1. \end{cases} \tag{10}$$

Also, $1/(1-\alpha)$ is negative if $\alpha > 1$ and positive if $\alpha < 1$. Hence, according to (7), and to the continuity for $\alpha = 1$, it results that, for every $\alpha > 0$,

$$N_{\alpha}(t) \geq 1. \tag{11}$$

Considering more specifically the case $\alpha = 0$, one can remark [6] that

$$\lim_{\alpha \to 0} M_{\alpha}(\mathbf{A}(t)) = \left(\prod_{k=1}^{K(t)} A_k(t) \right)^{\frac{1}{K(t)}} \tag{12}$$

which corresponds to the geometric means of the $K(t)$ components. If $A_k(t) > 0$ for every $k \in \{1, \ldots, K(t)\}$, the geometric means happens to be strictly positive and it follows from (8) that

$$\lim_{\alpha \to 0} N_{\alpha}(t) = K(t) \tag{13}$$

for any distribution of the amplitudes $\mathbf{A}(t)$. We will show in Section 4 that this theoretical result is however useless to deal with real data.

2.2.2. The 2-component case

In the 2-component case ($K(t) = 2$), one gets

$$N_{\alpha}(t) = \left(\frac{(1 + \rho^{\alpha}(t))^{\frac{1}{\alpha}}}{1 + \rho(t)} \right)^{\frac{\alpha}{1-\alpha}} \tag{14}$$

where $\rho(t) := A_1(t)/A_2(t)$. One can check that, if $\rho(t) = 1$, one gets $N(t) = 2$ for any α. Besides, for a given order α, one has $\lim_{\rho(t) \to \infty} N_{\alpha}(t) = 1$ and $\lim_{\rho(t) \to 0} N_{\alpha}(t) = 1$, whereas, for a given amplitude ratio $\rho(t)$, $\lim_{\alpha \to 0} N_{\alpha}(t) = 2$.

2.2.3. Confusing 2 or 3-component cases

In the 3-component case ($K(t) = 3$), one gets

$$N_{\alpha}(t) = \left(\frac{(1 + \rho_{12}^{-\alpha}(t) + \rho_{13}^{-\alpha}(t))^{\frac{1}{\alpha}}}{1 + \rho_{12}^{-1}(t) + \rho_{13}^{-1}(t)} \right)^{\frac{\alpha}{1-\alpha}} \tag{15}$$

where $\rho_{12}(t) := A_1(t)/A_2(t)$ and $\rho_{13}(t) := A_1(t)/A_3(t)$.

Eq. (15) permits to get an idea of the range of values of the amplitude ratios for which the estimed $N_{\alpha}(t)$ can be misleading in a 3-component situation. Indeed, assuming first for

simplicity that $\rho_{12}(t) = \rho_{13}(t) =: \rho(t)$, we get from (15) that $N_{\frac{1}{2}}(t) \leq 2 \Leftrightarrow \rho(t) \geq 16$ and $N_2(t) \leq 2 \Leftrightarrow \rho(t) \geq 4$. More generally, two examples of the generic behaviour of $N_\alpha(t)$ as a function of $\rho_{12}(t)$ and $\rho_{13}(t)$ are reported in Fig. 1, for the respective orders $\alpha = \frac{1}{2}$ and $\alpha = 2$.

It clearly appears that the estimated number of components $N_\alpha(t)$ is different from $K(t) = 3$ as soon as the ratio of the amplitude takes away from 1. Whenever $\rho_{12}(t) \neq \rho_{13}(t)$, the condition $N_\alpha(t) = 2$ defines three curves (reported as full blue lines in Fig. 1) that delineate regions where amplitude ratios may jointly lead to a misleading estimation of the number of components, ending up with a value $N_\alpha(t) < 2$ that, while stemming from a 3-component situation, might be compatible with a 2-component one.

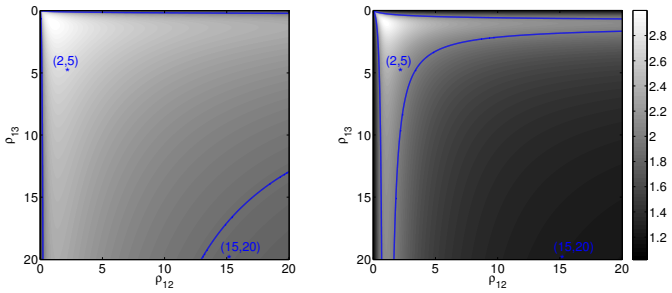

Fig. 1. Estimated number of components $N_\alpha(t)$ in the case $K(t) = 3$, as a function of the amplitude ratios $\rho_{12}(t)$ and $\rho_{13}(t)$, for a Rényi entropy of order $\alpha = \frac{1}{2}$ (left) and $\alpha = 2$ (right). The isocontours $N_\alpha(t) = 2$ are superimposed as full blue lines. The two specific cases that will be considered in Section 4 are reported as blue dots.

3. AN IMPROVED ALGORITHM

In the case of components with different amplitudes, the above analysis calls for a refining of the basic approach defined in [5]. Based on the results that $1 \leq N_\alpha(t) \leq K(t)$, we employ an iterative procedure in order to filter the dominant spectral component $\big($i.e., $\max_k A_k(t)\big)$ and thus to emphasize contributions from the weaker spectral components. Consequently, an index "i" is added to $N_\alpha(t)$ in order to denote the estimated number of components at each iteration of the algorithm, i.e., when a significative contribution is removed from the spectrogram.

The flowchart of the algorithm is given in Fig. 2. As in [5], the first term in the r.h.s. of (5) is estimated on a reference signal x_{ref} taken for simplicity as a pure tone. We denote $S_x(\theta, f)$ $\big($resp. $S_{x_{\text{ref}}}(\theta, f)\big)$ the spectrogram associated to the signal x (resp. x_{ref}). For real data, $S_x(\theta, f)$ is thresholded in order to remove part of the noise. The threshold value is a trade-off between the sensitivity of the algorithm to low energy components and false detection. The resulting

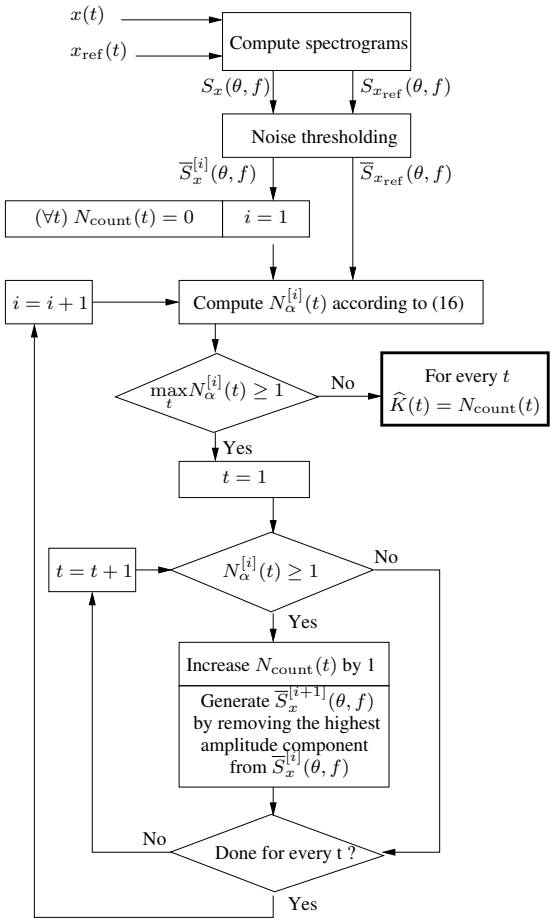

Fig. 2. Flowchart of the proposed algorithm.

spectrogram is denoted $\overline{S}_x^{[i]}(\theta, f)$.[1] At the i-th iteration, the estimated number of components is given by

$$N_\alpha^{[i]}(t) = 2^{H_{\alpha,x}^{[i]}(t) - H_{\alpha,x_{\text{ref}}}^{[i]}(t)} \tag{16}$$

where

$$H_{\alpha,x}^{[i]}(t) := \frac{1}{1-\alpha} \log_2 \int_{t-\frac{\Delta t}{2}}^{t+\frac{\Delta t}{2}} \int_{-\infty}^{+\infty} \left(\frac{\overline{S}_x^{[i]}(\theta, f)}{E_x^{[i]}} \right)^\alpha d\theta\, df \tag{17}$$

and $E_x^{[i]}(t) := \int_{t-\frac{\Delta t}{2}}^{t+\frac{\Delta t}{2}} \int_{-\infty}^{+\infty} \overline{S}_x^{[i]}(\theta, f)\, d\theta\, df$. Note that, in the algorithm, the removal from $\overline{S}_x^{[i]}(\theta, f)$ of the highest amplitude component is achieved within a cell of size $\Delta t \Delta f$.

Figure 3 presents the first four iterations of the proposed algorithm on a 3-component signal. We fix $\alpha = 2$ and, at each iteration i of the algorithm, $N_2^{[i]}(t)$ is computed. While $N_2^{[i]}(t) \geq 1$, the value $N_{\text{count}}(t)$ is increased by 1 and the

[1] The upper index $\cdot^{[i]}$ refers to the i-th iteration. $\overline{S}_x^{[i]}(\theta, f)$ denotes the spectrogram to be analyzed at the i-th iteration.

highest amplitude component is removed, by setting to zero $\overline{S}_x^{[i]}(\theta, f)$ around $f_k(t) = \arg\max_f \overline{S}_x^{[i]}(\theta, f)$, in order to generate $\overline{S}_x^{[i+1]}(\theta, f)$ from $\overline{S}_x^{[i]}(\theta, f)$. We denote $\widehat{K}(t)$ the final value of $N_{\text{count}}(t)$. This value denotes the estimate of $K(t)$ obtained with the proposed algortihm.

4. NUMERICAL EXPERIMENTS

Figure 4 compares the performance of the state-of-the-art method [5] with the proposed algorithm according to different signals: three simulated data and one real signal.

4.1. Theory versus numerical experiments

In this section, the spectrograms are computed with a Kaiser window of length 37 and $\Delta t = 11$.

The first experiment is designed in order to be close from the simplified model proposed in Section 2. Three components with different temporal lengths and with spectrogram amplitude ratios $\rho_{12} = 5$ and $\rho_{13} = 2$ are combined. As described in Figure 1, this situation is associated to the "non-confusing" one. As observed in the first column of Figure 4, the computation of $N_\alpha(t)$ with $\alpha = 1/2$ or $\alpha = 2$ leads to a good estimation of the number of component.

A similar experiment is presented in the second column with $\rho_{12} = 20$ and $\rho_{13} = 15$ (confusing 2-3-component situation, cf. Figure 1). This time, we clearly see the difficulty to observe a three component signal with the standard approach, while the proposed iterative algorithm succeeds in this task.

Before dealing with real data, we have run additive experiments in order to analyze AM-FM components. The results are presented in the third column of Fig. 4 and the good behavior of the proposed method, compared to the state-of-the art, is quite clear.

We can further observe that, when no threshold is applied on $S_x(\theta, f)$, using a too small α (here, $\alpha = 0.01$) leads to a bias in the computation of $N_\alpha(t)$. We therefore do not obtain the expected result $\lim_{\alpha\to 0} N_\alpha(t) = K(t)$ (cf. 2nd row and 1st, 2nd, and 3rd column in Figure 4), justifying from a different perspective the need of an improved algorithm.

4.2. Real data

The performance of the algorithm on real data is shown in the last column of Fig. 4. We deal in this case with a bat echolocation signal[2]. The spectrograms are computed with a Kaiser window of length 61 and $\Delta t = 3$. The results present some fluctuations, yet they stay in reasonable agreement with what can be expected from the spectrogram.

[2]The authors wish to thank Curtis Condon, Ken White, and Al Feng of the Beckman Institute of the University of Illinois for the bat data and for permission to use it in this paper.

5. CONCLUSION AND PERSPECTIVES

A methodology has been proposed and discussed for estimating the instantaneous number of components in a nonstationary multicomponent signal. This question is important because it is a necessary pre-processing step in advanced data-driven decomposition techniques such a synchrosqueezing [1] or Empirical Mode Decomposition [7].

Whereas it has been shown that a refined algorithm is effective for coping with situations that had not previously considered in [5] (unequal amplitudes), some questions still remain open. For instance, the role of the entropy index is better understood, but its choice could be made more objective, with the possibility of using this degree of freedom by means of a comparison between different estimations with different indices. Another point that has not been mentioned here is the influence of noise. Preliminary experiments tend to prove that the method is robust to moderate levels of additive noise, but this clearly needs to be further refined.

6. REFERENCES

[1] I. Daubechies, J. Lu, and H.-T. Wu. Synchrosqueezed wavelet transforms: An empirical mode decomposition-like tool. *Appl. Comp. Harm. Analysis*, 30(2):243–261, Mar. 2011.

[2] S. Meignen, T. Oberlin, and S. McLaughlin. On the mode synthesis in the synchrosqueezing method. In *Proc. European Signal Processing Conference*, pages 1865 – 1869, Bucharest, Romania, Aug. 27-31 2012.

[3] W.J. Williams, M.L. Brown, and A.O. Hero. Uncertainty, information, and time-frequency distributions. *Proc. Int. Soc. Opt. Eng.*, 1566:144–156, 1991.

[4] R.G. Baraniuk, P. Flandrin, A.J.E.M Janssen, and O. Michel. Measuring time-frequency information content using the Rényi entropies. *IEEE Trans. Inform. Theory*, 47(4):1391–1409, May 2001.

[5] V. Sucic, N. Saulig, and B. Boashash. Estimating the number of components of a multicomponent nonstationary signal using the short-term time-frequency Rényi entropy. *EURASIP Journal of Applied Signal Processing*, 125:1–11, 2011.

[6] G. Hardy, J.E. Littlewood, and G. Pólya. *Inequalities*. Cambridge Univ. Press, 1934.

[7] N. E. Huang, Z. Shen, S. R. Long, M. C. Wu, H. Shih, Q. Zheng, N.-C. Yen, C. C. Tung, and H. H. Liu. The empirical mode decomposition and the Hilbert spectrum for nonlinear and nonstationary time series analysis. *Proc. R. Soc. Lond. A*, 454:903–995, 1998.

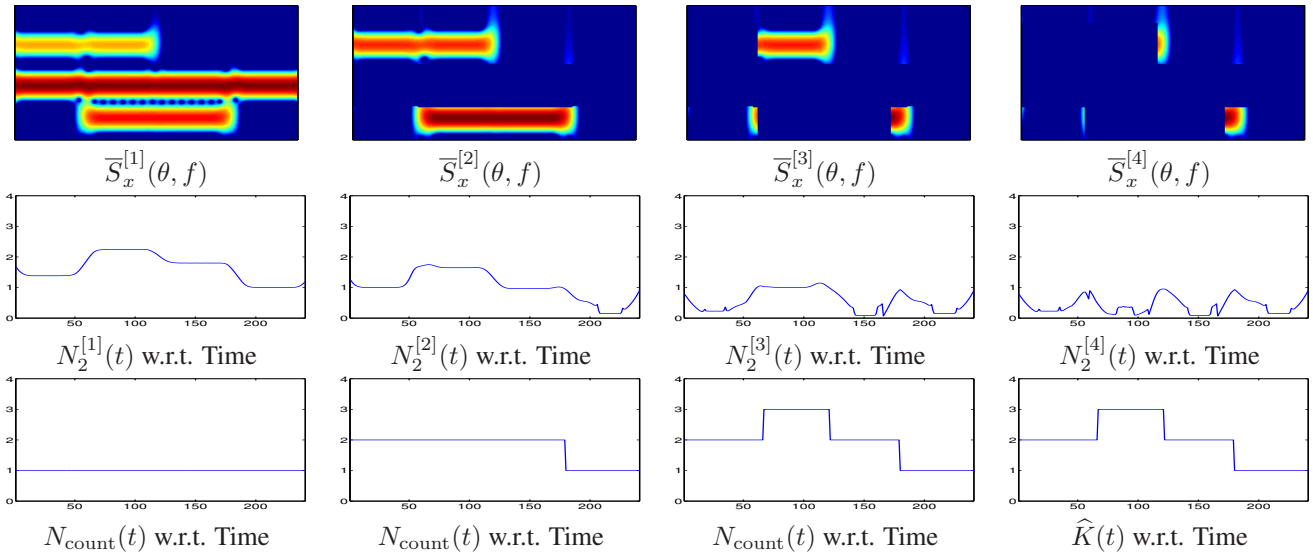

Fig. 3. Iterations of the proposed algorithm. Each column is associated to one iteration of the algorithm. The first row presents the spectrograms whose higher amplitude component is removed at each step. The second row shows the value N_α at the i-th iteration, based on the spectrogram. The third row is dedicated to the value $N_{\text{count}}(t)$. For the last iteration $N_{\text{count}}(t) = \widehat{K}(t)$.

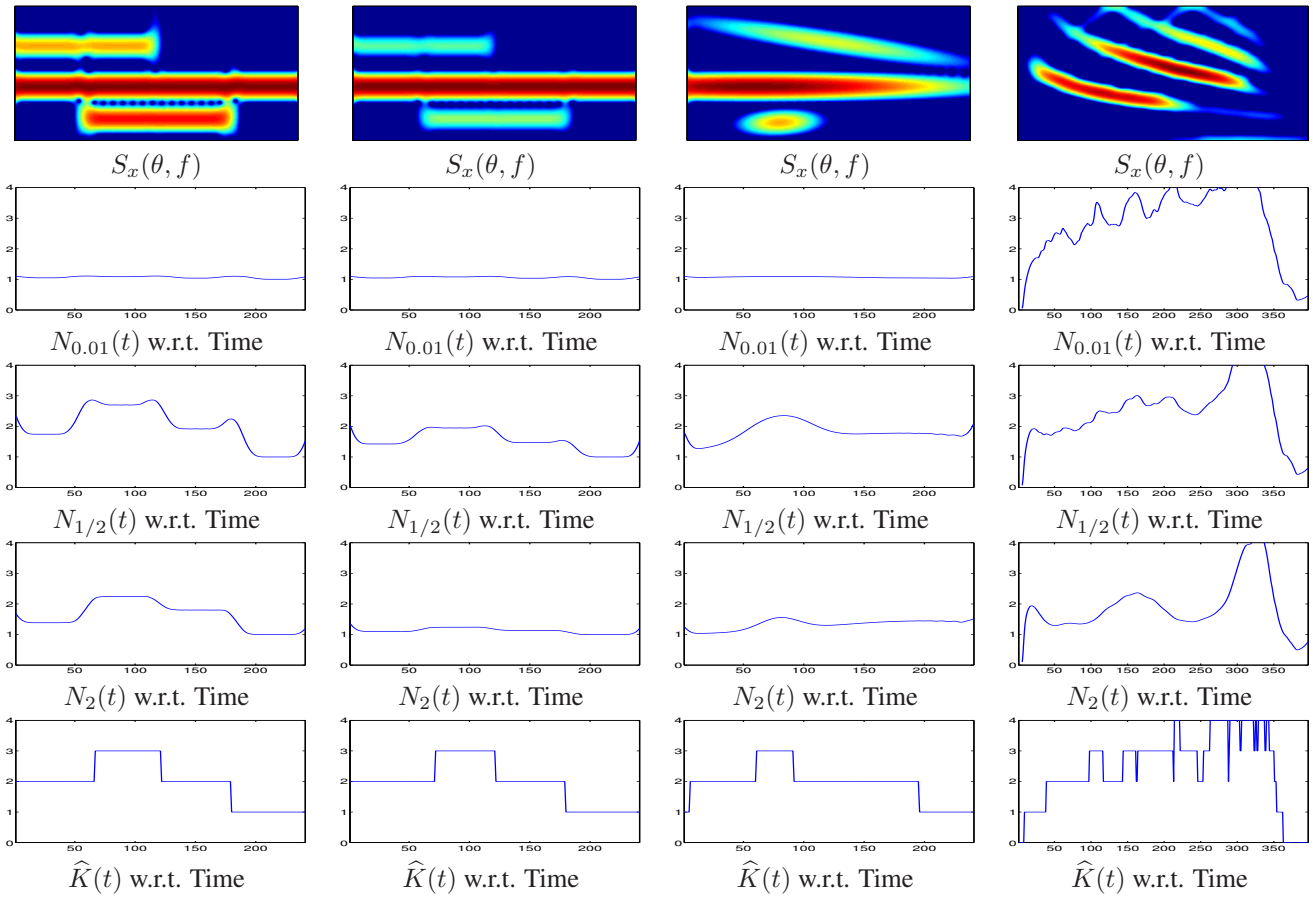

Fig. 4. Results obtained for different signals with the approach proposed in [5] with $\alpha = 0.01$ (2nd row), $\alpha = 1/2$ (3rd row), and $\alpha = 2$ (4th row) and with the proposed algorithm (5th row).